

CHEM MED CHEM

CHEMISTRY ENABLING DRUG DISCOVERY

Accepted Article

Title: Pyrrole-Based, Macrocyclic, Small-Molecule Inhibitors Targeting Oocyte Maturation

Authors: Jeong Kyu Bang, Pethaiah Gunasekaran, So Rim Lee, Seung-min Jeong, Jeong-woo Kwon, Toshiki Takei, Yuya Asahina, Geul Bang, Seongnyeon Kim, Mija Ahn, Eun Kyung Ryu, Hak Nam Kim, Ki-Yub Nam, Song Yub Shin, Hironobu Hojo, Suk Namgoong, and Nam-Hyung Kim

This manuscript has been accepted after peer review and appears as an Accepted Article online prior to editing, proofing, and formal publication of the final Version of Record (VoR). This work is currently citable by using the Digital Object Identifier (DOI) given below. The VoR will be published online in Early View as soon as possible and may be different to this Accepted Article as a result of editing. Readers should obtain the VoR from the journal website shown below when it is published to ensure accuracy of information. The authors are responsible for the content of this Accepted Article.

To be cited as: *ChemMedChem* 10.1002/cmdc.201700048

Link to VoR: <http://dx.doi.org/10.1002/cmdc.201700048>

WILEY-VCH

www.chemmedchem.org

A Journal of



Pyrrole-Based, Macrocyclic, Small Molecule Inhibitors Targeting Oocyte Maturation

Pethaiah Gunasekaran,^{[a]†} So-Rim Lee,^{[a]†} Seung-min Jeong,^[a] Jeong-Woo Kwon,^[a] Toshiki Takei,^[b] Yuya Asahina,^[b] Geul Bang,^[c] Seongnyeon Kim,^[c] Mija Ahn,^[d] Eun Kyung Ryu,^[d,g] Hak Nam Kim,^[d] Ki-Yub Nam,^[e] Song Yub Shin,^[f] Hironobu Hojo,^[b] Suk Namgoong,^{*[a]} Nam-Hyung Kim,^{*[a]} Jeong Kyu Bang^{*[d,g]}

- [a] Dr. P. Gunasekaran, S. Lee, S. M. Jeong, J.W. Kwon, Dr. S. Namgoong, Dr. N.H. Kim.
Molecular Embryology Laboratory, Department of Animal Sciences, Chungbuk National University, Chung-Buk 361-763, Republic of Korea
E-mail address: suknamgoong@chungbuk.ac.kr and nhkim@chungbuk.ac.kr
- [b] T. Takei, Dr. Y. Asahina, Dr. H. Hojo,
Institute for Protein Research, Osaka University, 3-2 Yamadaoka, Suita, Osaka, 565-0871, Japan
- [c] G. Bang, S. Kim
Biomedical Omics Group, Korea Basic Science Institute, Ochang, Chung-Buk 363-883, Republic of Korea
- [d] Dr. M. Ahn, Dr. E. K. Ryu, H. N. Kim, Dr. J. K. Bang
Division of Magnetic Resonance, Korea Basic Science Institute, Ochang, Chung-Buk 363-883, Republic of Korea
E-mail: bangjk@kbsi.re.kr
- [e] Dr. K.Y. Nam
Pharos I&BT Co., Ltd., Gyeonggi-do 14059, Republic of Korea
- [f] Dr. S.Y. Shin,
Department of Medical Science, Graduate School and Department of Cellular & Molecular Medicine, School of Medicine, Chosun University, Gwangju 501-759, Republic of Korea
- [g] Dr. E. K. Ryu, Dr. J. K. Bang
Department of Bio-analytical Science, University of Science & Technology, Daejeon, 34113, Republic of Korea.

† These authors are contributed equally

Abstract: Polo-like kinase 1 (Plk1) plays crucial roles in various stages of oocyte maturation. Recently, we reported that the peptidomimetic AB103-8 that targets polo box domain (PBD) of Plk1 affected oocyte meiotic maturation and meiosis resumption. However, to overcome the peptidic drawbacks, we designed and synthesized a series of pyrrole-based small-molecule inhibitors and screened against porcine oocyte maturation rates. Among them, macrocyclic compound **4** showed the highest inhibitory activity with enhanced inhibition against the embryos blastocyst formation. Furthermore, the addition of this compound to culture medium efficiently blocked the maturation of porcine and mouse oocytes, indicating that the lead compound could penetrate zona pellucida and cell membrane. To prove the Plk1 inhibition, we investigated this compound treated mouse oocytes which confirmed the Plk1 inhibition by showing impaired spindle formation. Finally, molecular modeling studies with Plk1 PBD also confirmed the presence of significant interactions between compound **4** and Plk1 PBD binding pockets, including phosphate, tyrosine-rich and pyrrolidine binding pockets. Collectively, these results suggest that the macrocyclic compound **4** may serve as a promising template for the development of novel contraceptive agents.

Introduction

Intracellular protein-protein interactions (PPIs) are playing essential roles in almost every cellular process, including DNA replication, transcription, translation, splicing, secretion, cell cycle control, and signal transduction.^[1-3] Similarly, such interactions serve a crucial role in the oocyte maturation process, for example, they are involved in the recognition and phosphorylation of Emi2 by polo-like kinase 1 (Plk1), and are crucial in controlling the cell cycle resumption. Recently, we demonstrated that one of our synthesized peptidomimetics, AB103-8, targeting the polo-box domain (PBD) of Plk1, inhibited the interaction between PBD and Emi2 that affected oocyte meiotic maturation and meiosis resumption.^[4] Hence, it is

evident that disrupting the specific interaction between PBD and Emi2 may be an attractive strategy for the development of novel contraceptive agents. In addition to lead peptidomimetics, AB103-8 was found to be successful in blocking oocyte maturation; however, the peptidic character of AB103-8 results in poor membrane permeability and protease stability, thereby hindering its development into a novel therapeutic.^[5] The enhancement of cell permeability can be achieved by converting them into conjugated peptides, such as a cell-penetrating peptide, or by PEGylation. However, these processes have complex routes of synthesis and can sometimes result in a great loss of activity.^[6] To overcome these problems, the design and synthesis of cell permeable, proteolytic non-hydrolysable, drug-like small-molecule inhibitors are highly imperative. The investigation of the structural parameters of AB103 series compounds (PDB ID 5DMJ) and related Plk1 PBD crystal structures (PDB ID 3RQ7) showed that the following three key functional moieties are required for effective interaction with Plk1 PBD: i) a broad pyrrolidine binding pocket surrounded by Trp414, Phe535, and Arg516, the binding of which determines the Plk1 selectivity among Plk2 and Plk3; ii) a deep and narrow tyrosine-rich channel, surrounded by Tyr417, Tyr481, and Tyr485, which are key for achieving a high binding affinity >1000 fold; and iii) a phospho binding pocket that interacts with His538 and Lys540 (Figure 1).^[7] Therefore, we envisioned the design and synthesis of a novel class of pyrrole-based, non-peptidic, cell-permeable, protease stable macrocyclic molecules for the efficient inhibition of oocytes.

The present work emerges as part of a research program that recently embarked on the development of oocyte maturation blocking studies^[4] and Plk1 PBD inhibitor synthesis.^[8-11] In this work, we have designed and synthesized an *N*-phenylalkyl

pyrrole-based macrocyclic inhibitor featuring phosphate residues on the alkyl side chain. To mimic AB103-8, we closely examined its binding in the crystal structure of P Plk 1 PBD in complex with **702** (PDB ID 5DMJ). The complex structure reveals that its long phenylalkyl residue was directed towards deep and narrow tyrosine-rich binding pockets,^[4] and that the phosphate group underwent a polar interaction with His538 and Lys540 at the phosphate binding pocket. We chose pyrrole residue as a core moiety, which can hold a flexible phenylalkyl chain linked at the NH position, and a variable alkyl chain bearing a phosphate moiety. Besides, deriving the macrocyclic structures in core moiety often result in the enhancement of protease stability.^[12]

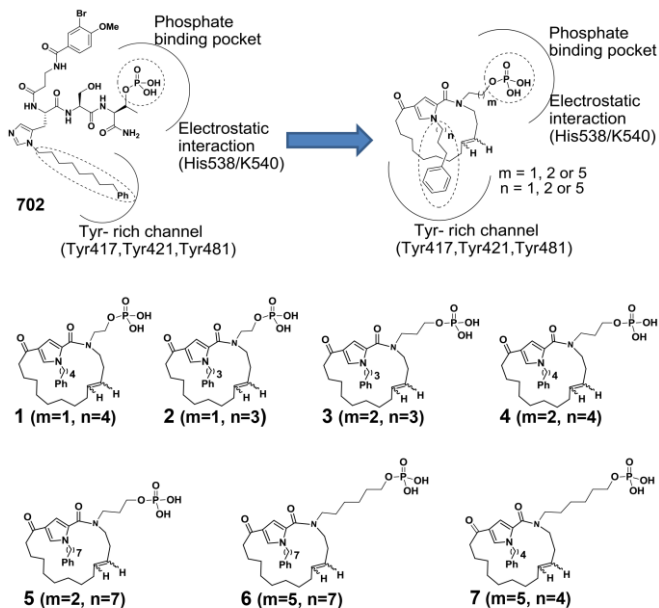


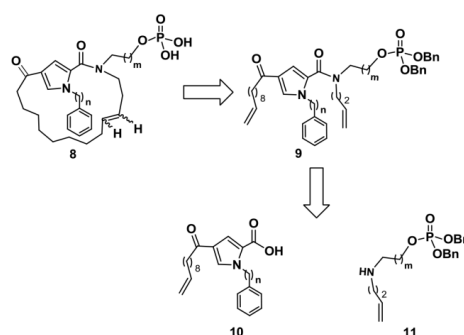
Figure 1. Binding nature of peptidomimetic **702** with Plk1 PBD and illustration of the cyclic molecule with all the synthesized compounds.

Thus, to the best of our knowledge, this is the first study to report a novel class of macrocyclic, non-peptidic, small molecules that effectively inhibit oocyte maturation. We synthesized a series of macrocyclic inhibitors by manipulating the alkyl lengths between the phenyl ring and pyrrole residue, and changing the alkyl chain length of the phosphate attached linker. These macrocyclic compounds were microinjected into immature porcine oocytes, and their potential to block *in vitro* oocyte maturation was compared with previously developed compound AB103-8 (positive control) and Bg34 (negative control). Among the synthesized compounds, the macrocyclic inhibitor compound **4** displayed the highest inhibition potential. To verify the Plk1 inhibition, spindle informations of compound **4** treated mouse oocytes were studied. Then, to analyze the binding nature of compound **4**, molecular models of Plk1 PBD and compound **4** complexes were generated by docking simulation and studied further.

Results and Discussion

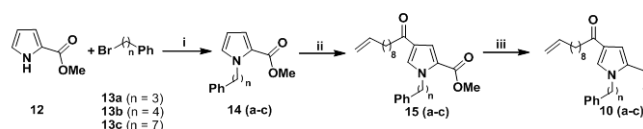
Chemistry

Based on the aforementioned preliminary structural prerequisites, we designed the *N*-phenylalkyl pyrrole-based macrocyclic molecule **8**, which features an alkyl phosphate group for binding with the phosphate binding pocket, and an *N*-phenylalkyl unit for targeting the deep and conserved tyrosine-rich channel, as shown in Figure 1. Retrosynthetic analysis suggested that macrocyclic small molecule **8** could be obtained from two terminal alkenic precursors, *N*-phenylalkyl pyrrole carboxylic acid (**10**) and the secondary amine (**11**) anchoring the phosphonate group, as outline in Scheme 1. The terminal diene **9** could be generated by amide coupling reaction of precursors **10** and **11**. Then, the ring-closing metathesis (RCM) reaction was performed for further cyclization, and subsequent benzylic deprotection of the phosphonate group would ultimately lead to the desired final compound.



Scheme 1. Retro synthetic pathway for the synthesis of macrocyclic compounds.

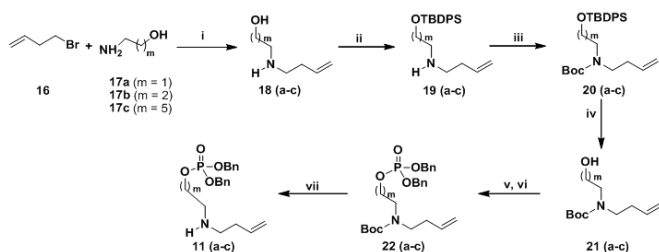
Our synthesis of **10** began with the incorporation of phenylalkyls at the nitrogen of pyrrole-2-methylester. *N*-alkylation of **12** was successfully carried out using various phenylalkyl bromides with different alkyl chain lengths, in the presence of NaH in dimethylformamide (DMF) (Scheme 2). To introduce the long alkenic chain at position 4 of the pyrrole residue, the Friedel-Crafts reaction was selected as a key tool to achieve the formation of **15** using 10-undecenoyl chloride and Yb(OTf)₃.^[13] Finally, the ester hydrolysis reaction was performed using KOH to yield the desired precursor **10** in good yields.



Scheme 2. Synthesis of **10**. Reagents and conditions: (i) NaH, DMF, 0 °C - rt ; (ii) 10-undecenoyl chloride, Yb(OTf)₃, CH₃NO₂, 0 °C - rt ; (iii) KOH, THF/EtOH/H₂O (9:1:1), reflux.

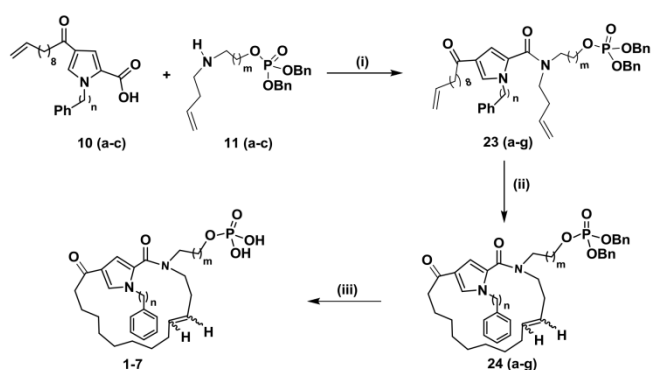
Next, the synthetic route for precursor **11** was developed using the initial coupling reaction of 4-bromo-1-butene (**16**) and respective amino alcohols **17** in the presence of NaI (Scheme 3) to yield **18**. Prior to achieving the phosphorylation of the hydroxyl group, the secondary amine must be protected to prevent undesirable reactions. Accordingly, the initial silyl protection of

the primary alcohol **19** was achieved in good yields using *tert*-butyldiphenylchlorosilane (TBDPSCI) in the presence of imidazole. Then, Boc-protection of the secondary amine was performed using (Boc)₂O in the presence of triethylamine and 4-dimethylaminopyridine (DMAP). To recover the alcohol functional group, deprotection of the primary alcohol was effected in the presence of tetrabutylammonium fluoride (TBAF) in tetrahydrofuran (THF) to yield alcohol **21**.^[14]



Scheme 3. Synthesis of **11**. *Reagents and conditions:* (i) NaI, MeOH, reflux; (ii) TBDPSCI, Imidazole, THF, rt; (iii) (Boc)₂O, DMAP, Et₃N, CH₂Cl₂, rt; (iv) TBAF, THF, rt; (v) dibenzyl *N,N*-diisopropyl phosphoramidite, 1*H*-tetrazole, rt; (vi) *m*-CPBA, rt; (vii) TFA/CH₂Cl₂ (1:6), rt.

Then, the alcohol was phosphorylated using dibenzyl-*N,N*-diisopropylphosphoramidite in the presence of 1*H*-tetrazole, and the subsequent oxidation in the presence of *m*-chloroperoxybenzoic acid (*m*-CPBA) resulted in the benzyl-protected phosphoryl ester **22**.^[11] Finally, TFA-mediated Boc (*t*-butyloxycarbonyl) deprotection of the secondary amine resulted in the formation of desired precursor **11**. After the successful synthesis of precursors **10** and **11**, our next objective was to enable the amide coupling reaction using 2-(1*H*-benzotriazol-1-yl)-1,1,3,3-tetramethyluronium hexafluorophosphate (HBTU) and *N,N*-diisopropylethylamine (DIEA) in DMF to achieve diene **23** in good yields (Scheme 4). Then, the two terminal alkenes of **23** underwent the RCM reaction in order to enable the cyclization process using the Grubbs 2nd generation catalyst.^[15] Finally, the removal of the benzyl group from the phosphonate ester was effected in the presence of TFA/TIS/H₂O (10:1:1) to obtain the desired final compounds. Following the above methodology, further derivatization of macrocyclic compounds, **1-7** was achieved by manipulating the alkyl chain lengths of the phenyl and phosphate linkers.



Scheme 4. Synthesis of compounds **1-7**

Reagents and conditions: (i) HBTU, DIEA, DMF, rt; (ii) Grubbs 2nd gen. DCM, 45 °C; (iii) TFA/TIS/H₂O (10:1:1), rt.

Biological evaluations

Having developed the synthetic protocol for the facile synthesis of the targeted molecule, we then tested the effect of our macrocyclic compounds on porcine oocyte maturation rates, as shown in Figure 2A. The synthesized macrocyclic inhibitors **1-7** were screened for porcine oocyte maturation rates along with the peptidomimetics AB103-8 (positive control) and Bg34 (negative control), and subjected to *in vitro* maturation for 44h. The majority of the macrocyclic compounds exhibited a significant effect on the maturation rate of porcine oocytes.

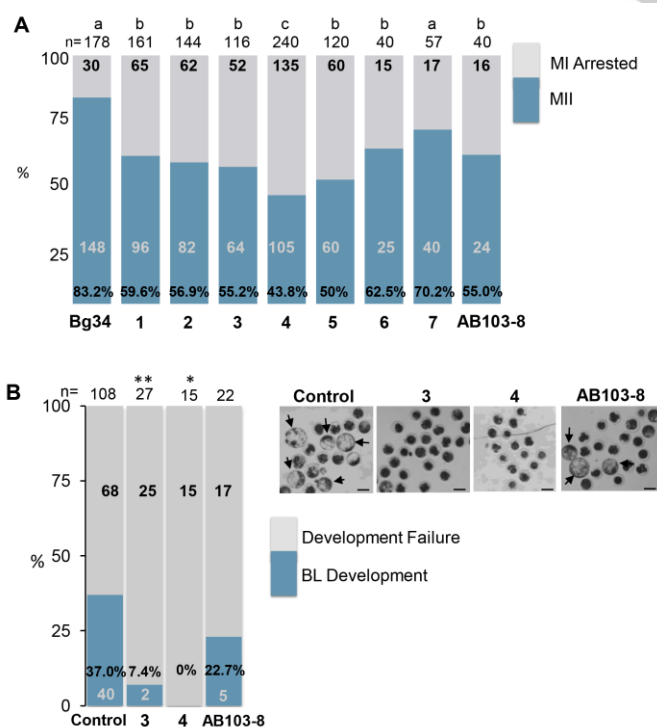


Figure 2. Microinjection of macrocyclic compounds on porcine oocytes impairs oocyte maturation and pathernogenic embryo developments.

A. Inhibition of porcine oocyte maturation by microinjections of macrocyclic compounds (**1-7**). Percentage of oocytes matured to metaphase II (MII) against total oocytes were plotted. Numbers of oocytes per each treatment groups were indicated on the top of the graph. Oocyte failed to reach MII stage were defined as 'MI arrested', while oocyte extruded polar body were counted as 'MII'. Statistically significant differences ($p < 0.05$, ANOVA) in oocyte maturation rates are indicated by a different superscript letters (a,b and c).^[16]

B. Failure of pathernogenic embryo developments caused by microinjection of macrocyclic compounds: Oocytes injected with macrocyclic compounds (**3** or **4**), control chemicals (AB103-8) and non-injected control reached MII stages were subjected to pathernogenic activations and their developments to blastocyst stages were monitored and plotted. Embryo developed until blastocyst stages were counted as 'BL Developments' and embryos did not reach to blastocyst was classified as 'Development Failure'. Number of embryos per each treatment groups was indicated on the top of the plot. Significant differences between the treatment groups and the control group are indicated by an asterisk ($***P \leq 0.001$, $**P \leq 0.01$, $*P \leq 0.05$). Arrows indicate blastocysts developed. Scale bar: 120 μ m.

Firstly, compounds, **1** and **2**, were attached with butylphenyl and propylphenyl, respectively, and the phosphate linker was connected with ethyl chain. During the screening of porcine oocyte maturation rates, these compounds showed a slight decrease in inhibition rates (**1**: 59.6%, and **2**: 56.9%) compared with that of the positive control, AB103-8 (55.0%). The extension of the phosphate linkers in **1** and **2**, from ethyl to a propyl chain, resulted in the formation of **4** and **3**, respectively. Further examination of these compounds on porcine oocyte maturation rates reveals that compound **4** was found to exhibit effective inhibitory activity (maturation rate, 43.8%, 105/240), which was significantly higher compared with that of the negative control Bg34 (83.2%, 148/178, $p < 0.001$). Meanwhile, compound **3** showed an inhibition rate similar to that of the peptidomimetic AB103-8 (55.2 %). It is evident from the above results that variation in the chain lengths of the phosphate linker alters the inhibition rate of the macrocyclic compounds in porcine oocyte maturation.

Next, to investigate the effect of the phenylheptyl attached to AB103-8 that targets the tyrosine-rich channel, we modified **4** by attaching the phenylheptyl chain at the pyrrole residue leading to the formation of the inhibitor, **5**. Unfortunately, the change in phenylalkyl chain length did not result in any improvements in the porcine oocyte maturation inhibition rate (50%). Instead, it was found to display reduced inhibition rates compared with that of the most effective compound, **4**. To further determine the effect of increasing the chain lengths of the phosphate linker on the inhibition rate, we further extended the chain lengths from propyl to hexyl chains, resulting in compounds **6** and **7**. In these compounds, the pyrrole remained connected to the phenylheptyl and phenylbutyl chains, respectively. In contrast to the previous results, macrocyclic compounds **6** and **7** resulted in reduced oocyte maturation rates, at 62.5% and 70.2%, respectively. Thus, compound **4** was found to be most effective inhibitor of porcine oocytes maturation rates.

Although the injection of macrocyclic compounds decreased oocyte maturation efficiency, significant proportions of oocytes still managed to extrude the polar body to evolve as a matured oocyte. Therefore, we tested the embryonic developmental potential of these oocytes, which managed to develop until metaphase II (MII). Following the injections of a macrocyclic compound (**3** or **4**) or AB103-8, the oocytes were subjected to *in vitro* maturation. Then, the MII-stage oocytes were subjected to parthenogenetic activation by electric shock in order to induce embryonic development. As shown in Figure 2B, the blastocyst formation rate of parthenogenetically activated oocytes injected with **3** or **4** macrocyclic compounds was nearly abolished (**3**: 2/27, $p < 0.01$; **4**: 0/15, $p < 0.05$), which was in contrast to that of oocytes injected with the control (37%, 40/108) or AB103-8 (23%, 5/22). These results prove that macrocyclic compounds inhibit porcine oocyte maturation and further affect embryonic development potential.

In contrast to the peptidomimetic AB103-8, macrocyclic compounds have hydrophobic properties, so we tested the hypothesis that the macrocyclic compounds could penetrate the zona pellucida and oocyte membrane of porcine. To facilitate the screening, we added each macrocyclic compound, at a concentration of 10 μ M, to the culture media for the *in vitro* maturation of porcine oocytes and assessed their effects on oocyte maturation by comparing with peptidomimetic AB103-8 and Bg34. As shown in Figure 3A, the addition of 10 μ M

macrocyclic compounds significantly decreased the porcine oocyte maturation rate, similar to the results obtained using direct microinjections of compounds in cytoplasm. In this screening, compound **4** was found to be the most effective compound at inhibiting oocyte maturation rates (30.3%, 61/201, $p < 0.001$) compared with that of the control Bg34 (84.0%, 278/331), and AB103-8 (65%, 118/179). This result proves that the most potent compound **4** is highly permeable than that of the peptidomimetics AB103-8. And also this consistency in the results of **4** indicates that macrocyclic compounds can penetrate zona pellucida and oocyte cell membranes, and consequently negatively affect oocyte maturation.

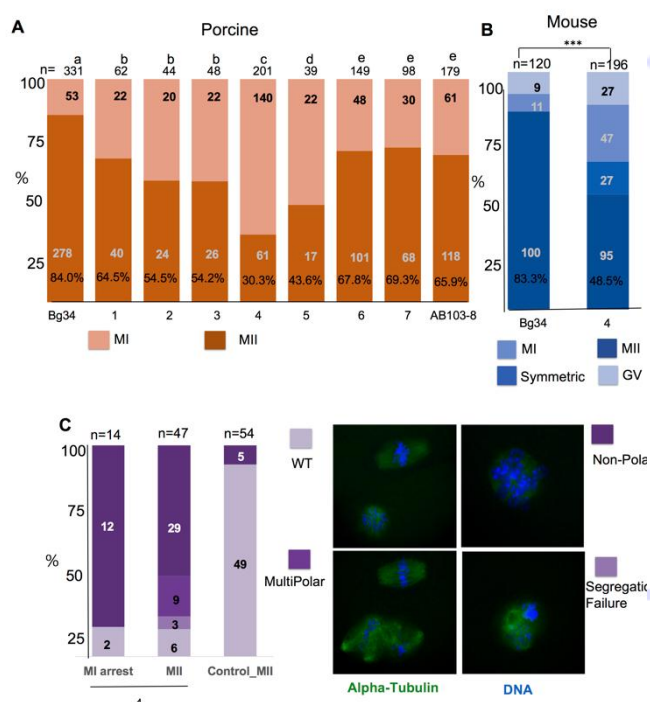


Figure 3. The inclusion of macrocyclic compounds in culture media impairs porcine and mouse oocyte maturation.

A. Inhibition of porcine oocyte maturation by macrocyclic compounds was supplemented in culture medium at 10 μ M of concentration. Percentage of oocytes matured to metaphase II (MII) against total oocytes were plotted. Numbers of oocytes per each treatment groups were indicated on the top of the graph. Oocyte failed to reach MII stage were defined as 'MI arrested', while oocyte extruded polar body were counted as 'MII'. Statistical differences ($p < 0.05$, ANOVA) between different treatments are indicated by a different superscript letters (a, b, c, d and e). **B.** Failure of mouse oocyte maturation by macrocyclic compound, **4** treatments: 10 μ M of macrocycles and control chemicals were supplemented in the medium during *in vitro* maturation. Oocyte growth stages after 12 h of *in vitro* maturation were classified and counted; GV: Oocytes failed to undergo germinal vesicle (GV) breakdown; MI: Oocytes had undergone to GV breakdown, but failed to extrude polar body; Symmetric: Oocytes had undergone cytokinesis, but have unusually bigger polar body (classified with polar body which has more than 50% of diameter of that of oocyte); MII: Oocytes had undergone polar body extrusion and had normal polar body. Significant differences between the treatment groups and the control group are indicated by an asterisk (** $P \leq 0.01$, * $P \leq 0.05$). **C.** Meiotic spindles in oocytes treated with **4** were stained with alpha-tubulin (Green) and DAPI for DNA (Blue). Oocytes failed with polar body extrusion (MI arrest) and oocytes protruded polar body (MII) were classified

separately. Each oocyte was classified as wild type (WT), non-polar spindle (Non-Polar), multipolar spindle (MultiPolar), and Segregation Failure and counted.

Then, in order to investigate the ability of macrocyclic compounds in inhibiting other mammalian oocyte maturation, we tested the inhibitory potential of **4** in mouse oocyte maturation. As presented in Figure 3B, the addition of **4** to *in vitro* culture medium at 10 μ M concentration significantly decreased mouse oocyte maturation rates (48.5%, $n=95/196$; $p<0.001$) compared with that of the control (83.3%, $n=100/120$). Treatment of **4** compound also increases the fraction of oocytes with the large polar body (13.7%, $n=27/196$), which have polar body bigger than 50% of oocyte's diameter, while none of oocyte without chemical treatments showed abnormally large polar body (0%, $n=0/120$). Considering that bigger polar body or failure of asymmetric division is caused by spindle migration defect,^[17] these results suggest that treatment with **4** negatively affects spindle migration during oocyte maturation.

In order to examine the Plk1 inhibiting ability of the lead compound, we analyzed the meiotic spindles in compound **4** treated mouse oocytes. It is previously reported that the inhibition of Plk1 in mouse oocytes causes the impairment of the microtubule organization center (MTOC), and therefore results in problems regarding meiotic spindle formation.^[18] It is pertinent to note that the meiotic spindles in **4**-treated mouse oocytes are consisted of major portions of abnormal meiotic spindles compared with that of wild-type oocytes (Figure 3C). For instance, the majority of control MII-stage oocytes had typically normal bipolar spindles (91%, 49/54). However, **4** treated oocyte displayed only a small fraction of bipolar spindles (14%, 2/14 in MI-arrested oocytes; 13%, 6/47 in MII-stage oocytes). Moreover, most of the **4** treated meiotic spindles in mouse oocytes displayed non-polar morphology (86%, 12/14 in MI arrested oocytes; 62%, 29/47 in MII-stage oocytes). In addition, **4** treated oocytes in MII-stage also displayed the multipolar spindles (19%, 9/47). These results firmly suggest that treatment with compound **4** impair the formation of meiotic spindles during

mouse oocyte maturation. Considering previously described roles of Plk1 in meiotic spindle formation,^[17] the results from the present study strongly suggest that the inhibitory effect of macrocyclic compound **4** results in the inhibition of Plk1, and therefore cause depletion of MTOC formation.

Molecular Modelling

To gain molecular insight into the ligand binding site interactions responsible for the inhibitory effect of macrocyclic compound **4** in oocyte maturation studies, we investigated the binding interactions of molecular modeling structure of the Plk1 PBD and compound **4** complexes (Figure 4). The molecular modeling results of the Plk1 PBD and compound **4** complexes revealed that three primary binding interactions were present between the macrocyclic compound, **4**, and Plk1 PBD. The initial inference of molecular docking results revealed that there were tight charge-charge interactions between the phosphate group of **4** and the two positively charged residues, His538 and Lys540, in the phosphate-binding region. Secondly, the four carbon tethered phenyl alkyl unit of **4** were projected towards the narrow passage of the tyrosine-rich hydrophobic channel to exert hydrophobic interactions, as shown in Figure 4. These two interactions are identical to that of the AB103-8-related compound **702** binding the Plk1 PBD complex (PDB ID 5DMJ). In addition to the above interactions, the pyrrole ring in compound **4** is bound to the pyrrolidine binding pocket through an effective π - π -stacking interaction that exists between the pyrrole ring of compound **4** and the side-chain of Trp414. Furthermore, the ethylene moiety present in the macrocyclic ring of compound **4** showed contact with the side chain of Phe535. Finally, the carbonyl group that connected directly with the fourth position of the pyrrole residue in the macrocyclic compound, **4**, showed weak hydrogen bonding interactions, with a backbone N-H of Asp416. It is expected that the additional interactions exhibited by compound **4** may be instrumental factors in its superior activity in oocyte maturation, compared with AB103-8.

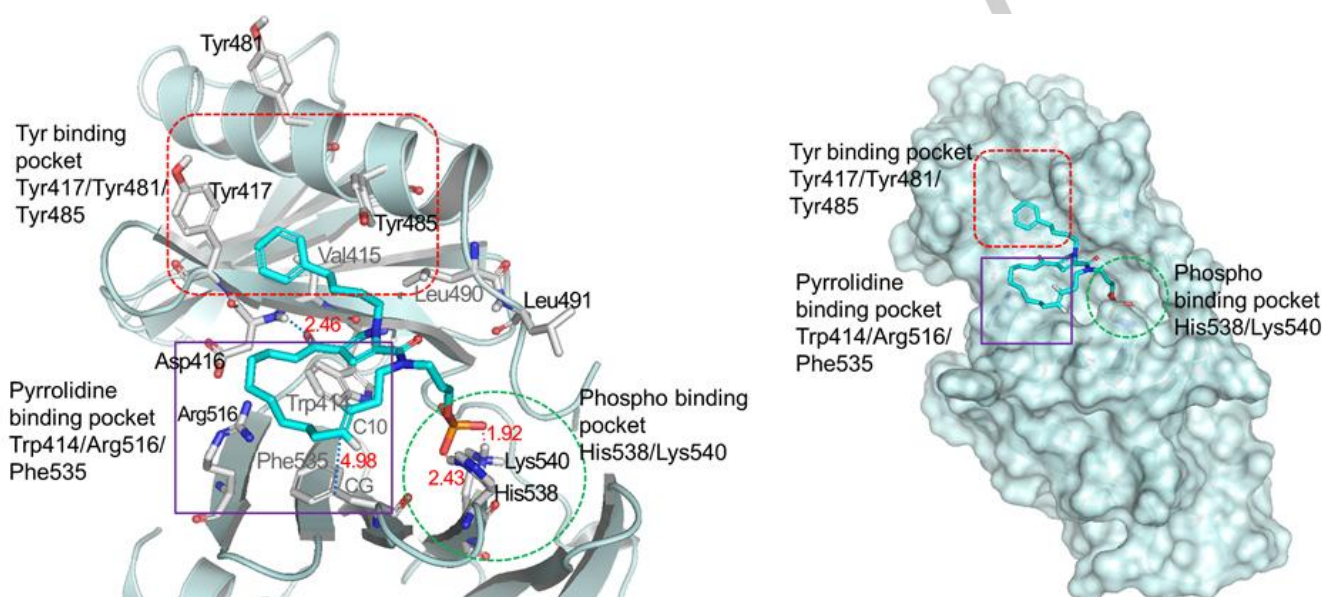


Figure 4. Modeling structure of the Plk1 PBD and **4** complexes, which shows the presence of the phosphate binding pocket, pyrrolidine-binding pocket and Tyr-rich hydrophobic channel. Modeling structure was generated using Pymol (<http://www.pymol.org>)

Conclusions

This study demonstrates the efficient design and synthesis of pyrrole-based, macrocyclic, small molecule inhibitors that are more effective than previously reported peptidomimetics, such as AB103-8, in inhibiting oocyte maturation. The synthesized molecules were successfully screened for their effects on porcine oocyte maturation rates, and the macrocyclic inhibitor **4** was found to have good inhibitory potential against oocyte maturation. In addition, this inhibitor was found to prevent embryonic development, indicating that compound, **4** treatment could block mammalian early embryogenesis in addition to oocyte maturation. It has been reported that the inhibition of Plk1, by kinase-domain inhibitor BI2536 or morpholino antisense oligonucleotide, can block the early embryogenesis of zebrafish,^[19] indicating the importance of Plk1 in the early embryogenesis of vertebrae. Moreover, **4** treated mouse oocyte was found to show the impaired mouse spindles, suggesting that there is Plk1 inhibition. These results suggest that Plk1 would be an effective target for the development of novel contraceptive drugs. We also confirmed that **4** could effectively block oocyte maturation when it was added to oocyte culture media at 10 μ M. The hydrophobic nature of this inhibitor may explain its ability to penetrate the zona pellucida and cell membrane. Finally, molecular modeling of Plk1 PBD and **4** complexes revealed that the primary binding interactions in the regions, including the phospho binding pocket, tyrosine-rich channel, and pyrrolidine binding pocket, along with additional interactions, may be a critical factor in its ability to more effectively inhibit oocyte maturation, in comparison with the peptidomimetic AB103-8. Hence, the macrocyclic compound **4** could represent a model for developing novel contraceptive agents.

Experimental Section

Chemistry

All reagents and starting materials were obtained from commercial chemical suppliers (Sigma-Aldrich or TCI) and used as received. Anhydrous organic solvents were purchased from Aldrich and used directly. Thin layer chromatography (TLC) was performed on Merck aluminum sheets with silica gel 60 F254 and were visualized by ultraviolet light and staining with KMnO_4 . Column chromatography was performed on Merck silica gel 60 (70-230 mesh or 230-400 mesh). ^1H and ^{13}C NMR spectra were recorded on a Bruker DRX-400 and DRX-500 spectrometer. Chemical shifts (δ) are reported in parts per million (ppm) measured relative to an internal standard and coupling constants (J) are expressed in hertz (Hz). All final compounds (**1-7**) were purified by preparative reverse-phase high performance liquid chromatography (RP-HPLC) and judged to be $\geq 95\%$ pure by analytical HPLC equipped with C_{18} column (4.6 \times 250 mm, 10 microns). Two different linear gradients of 0.05% aq. TFA (eluent A) and 0.05% TFA in CH_3CN (5-95/30 min, eluent B) were used with a flow rate of 1.0 mL/min at 25 $^\circ\text{C}$. The synthesized compounds were confirmed by ESI-MS, HRMS, and MALDI-TOF mass spectrometer (Shimadzu).

General Procedure A for the synthesis of 14a-14c

methyl 1-(3-phenylpropyl)-1H-pyrrole-2-carboxylate (**14a**)

NaH (60% w/w in mineral oil, 102 mg, 2.55 mmol) was added to a stirred solution of methyl 1H-pyrrole-2-carboxylate (**12**) (200 mg, 1.59 mmol) in DMF (20 mL) at 0 $^\circ\text{C}$. After stirring at room temperature for 30 min, 3-phenylpropyl bromide (**13a**) (324 mg, 1.63 mmol) was added slowly at 0 $^\circ\text{C}$. The temperature was slowly raised to room temperature

and stirred for 4 h. Then the reaction mixture was treated with saturated aqueous NH_4Cl (10 mL) and extracted with ethyl acetate (30 mL). The combined organic extracts were washed with water (3 \times 15 mL) and brine, dried over Na_2SO_4 , and evaporated. The crude product was purified by silica gel column chromatography (hexane-ethyl acetate, 20:1) to afford **14a** as colourless oil (248 mg, 64%).

methyl 1-(4-phenylbutyl)-1H-pyrrole-2-carboxylate (**14b**)

Compound **14b** was synthesized from methyl 1H-pyrrole-2-carboxylate (**12**) and 4-phenylbutyl bromide (**13b**) following the general procedure A (colourless oil, 69%)

methyl 1-(7-phenylheptyl)-1H-pyrrole-2-carboxylate (**14c**)

Compound **14c** was synthesized from methyl 1H-pyrrole-2-carboxylate (**12**) and 7-phenylheptyl bromide (**13c**) following the general procedure A (colourless oil, 62%)

General Procedure B for the synthesis of compound 15a-15c methyl 1-(3-phenylpropyl)-4-undec-10-enoyl-1H-pyrrole-2-carboxylate (**15a**)

To a stirred solution of 10-undecenoyl chloride (728 mg, 2.12 mmol) and $\text{Yb}(\text{OTf})_3$ (101.6 mg, 0.164 mmol) in nitromethane at 0 $^\circ\text{C}$ was added **14a** (400 mg, 1.64 mmol) slowly. The resulting reaction mixture was stirred at room temperature for 18 h. The reaction was quenched with saturated aqueous NaHCO_3 (15 mL) and the mixture was extracted with diethyl ether (3 \times 15 mL). The organic layers were washed with water and brine, dried over Na_2SO_4 and volatiles were removed under vacuo. The resultant residue was purified by silica gel column chromatography (hexane-ethyl acetate, 20:1) to afford **15a** as colourless oil (281 mg, 42%).

methyl 1-(4-phenylbutyl)-4-undec-10-enoyl-1H-pyrrole-2-carboxylate (**15b**)

Compound **15b** was synthesized from compound **14b** and 10-undecenoyl chloride in the presence of $\text{Yb}(\text{OTf})_3$ following the general procedure B (colourless oil, 44 %).

methyl 1-(7-phenylheptyl)-4-undec-10-enoyl-1H-pyrrole-2-carboxylate (**15c**)

Compound **15c** was synthesized from compound **14c** and 10-undecenoyl chloride in the presence of $\text{Yb}(\text{OTf})_3$ following the general procedure B (colourless oil, 41 %).

General Procedure C for the synthesis of compound 10a-10c

1-(3-phenylpropyl)-4-undec-10-enoyl-1H-pyrrole-2-carboxylic acid (**10a**)

To a solution of **15a** (650 mg, 1.59 mmol) in THF/EtOH (20 mL (6:1)) was added potassium hydroxide (711 mg, 12.71 mmol) in water (3 mL). The resulting reaction mixture was refluxed for 12 h and cooled to room temperature. Then the reaction mixture solvents were removed under vacuo, and the residue in water was acidified to pH 1 using 32% aqueous HCl. The resultant precipitate was filtered and washed with water to obtain the carboxylic acid as a yellow sticky solid **10a** (464 mg, 74%).

1-(4-phenylbutyl)-4-undec-10-enoyl-1H-pyrrole-2-carboxylic acid (**10b**)

Compound **10b** was synthesized from compound **15b** using potassium hydroxide following the general procedure C (yellow solid, 79 %).

1-(7-phenylheptyl)-4-undec-10-enoyl-1H-pyrrole-2-carboxylic acid (**10c**)

Compound **10c** was synthesized from compound **15c** using potassium hydroxide following the general procedure C (yellow solid, 79 %).

General Procedure D for the synthesis of compound 19a-19c M-[2-(tert-butyl) diphenylsilyloxy]ethyl]but-3-en-1-amine (**19a**)

To a stirred solution of **16** (1.00 g, 7.40 mmol) and 2-aminoethanol (**17a**) (1.58 mL, 22.2 mmol) in MeOH (30 mL) was added NaI (0.27 g, 1.85 mmol). The resultant reaction mixture was refluxed for 3 h. Then the reaction mixture was cooled to room temperature and evaporated under

vacuo. The residue was treated with saturated aqueous NH_4Cl solution and ethyl acetate. After the separation of the two layers, the aqueous layer was basified with 40% sodium hydroxide and extracted with ethyl acetate. The combined organic layers were dried over Na_2SO_4 and concentrated under vacuo to afford **18** (0.84 g, 100% yield) as a colourless viscous oil. This crude oil was used for the next step by dissolving in THF (50 mL), to which TBDPSCI (4.06 g, 1.48 mmol) and imidazole (1.1 g, 16.3 mmol) were added, and stirred for 14 h at room temperature. The reaction mixture was evaporated under vacuo, and the residue was purified by silica gel column chromatography (hexane-ethyl acetate, 3:7) to provide **19a** (2.45 g, 94 %) as a colourless oil.

N-3-(*tert*-butyldiphenylsilyloxy)propyl)but-3-en-1-amine (**19b**)

Compound **19b** was synthesized from **16** and **17b** in the presence of NaI following the general procedure D (colourless oil, 76 %).

N-(but-3-enyl)-6-(*tert*-butyldiphenylsilyloxy)hexan-1-amine (**19c**)

Compound **19c** was synthesized from **16** and **17c** in the presence of NaI following the general procedure D (colourless oil, 76 %).

General Procedure E for the synthesis of compound 20a-20c

tert-butyl but-3-enyl(2-(*tert*-butyldiphenylsilyloxy)ethyl)carbamate (**20a**)

(Boc)₂O (0.495 g, 2.27 mmol) was added to a solution of **19a** (0.4 g, 1.13 mmol), triethylamine (3.8 mL, 2.66 mmol), and 4-dimethylaminopyridine (DMAP) (0.05 g, 0.44 mmol) in dichloromethane (DCM) (100 mL) at 0 °C. The reaction mixture was allowed to stir at room temperature for 14 h. The resultant reaction mixture was washed with brine, dried (Na_2SO_4) and concentrated under vacuo. The crude product was purified by flash column chromatography (hexane-ethyl acetate, 20:1) to afford **20a** (0.451 g, 88 %) as a colourless oil.

tert-butyl but-3-enyl(3-(*tert*-butyldiphenylsilyloxy)propyl)carbamate (**20b**)

Compound **20b** was synthesized from **19b** using (Boc)₂O, triethylamine, and DMAP following the general procedure E (colourless oil, 94 %).

tert-butyl but-3-enyl(6-(*tert*-butyldiphenylsilyloxy)hexyl)carbamate (**20c**)

Compound **20c** was synthesized from **19c** using di-*tert*-butyldicarbonate, triethylamine, and DMAP following the general procedure E (colourless oil, 84 %).

General Procedure F for the synthesis of compound 21a-21c

tert-butyl but-3-enyl(2-hydroxyethyl)carbamate (**21a**)

To a stirred solution of **20a** (0.5 g, 1.10 mmol) in THF (50 mL) at 0 °C was added *n*-tetrabutylammonium fluoride (TBAF) (1.0 M in THF) (1.33 mL, 1.33 mmol). The reaction mixture was warmed to room temperature and stirred for 14 h. Then the reaction mixture was concentrated under vacuo. The resulting residue was re-suspended in diethyl ether (80 mL) and washed with water (40 mL). The aqueous layer was extracted again with diethyl ether. The combined organic extracts were dried (Na_2SO_4) and concentrated. The crude residue was purified by flash column chromatography (hexane-ethyl acetate, 6:4) to afford **21a** (0.18 g, 76 %) as a colourless oil.

tert-butyl but-3-enyl(3-hydroxypropyl)carbamate (**21b**)

Compound **21b** was synthesized from **20b** using *n*-tetrabutylammonium fluoride(TBAF) following the general procedure F (colourless oil, 95 %).

tert-butyl but-3-enyl(6-hydroxyhexyl)carbamate (**21c**)

Compound **21c** was synthesized from **20c** using *n*-tetrabutylammonium fluoride(TBAF) following the general procedure F (colourless oil, 92 %).

General Procedure G for the synthesis of compound 22a-22c

tert-butyl 2-(bis(benzyloxy)phosphoryloxy)ethyl(but-3-enyl)carbamate (**22a**)

To a mixture of **21a** (1.65 g, 7.67 mmol) and 0.45 M acetonitrile solution of tetrazole (51 mL, 23 mmol) was added dibenzyl *N,N*-

diisopropylphosphoramidite (5.2 g, 15.3 mmol) at 0 °C. The resulting solution was stirred at room temperature for 4 h. Then, *m*-CPBA (1.98 g, 11.5 mmol) was added to the reaction mixture at 0 °C, and the reaction mixture was stirred for further 1 h at room temperature. Then the precipitate was filtered and washed with dichloromethane (30 mL). The filtrate was concentrated under vacuo and resuspended in dichloromethane (50 mL). The combined dichloromethane solutions were washed with a saturated aqueous NaHCO_3 and brine. The organic layer was dried over sodium sulfate, filtered, and concentrated under vacuo. The residue was purified by flash column chromatography (diethyl ether-hexane, 1:1) to provide **22a** (3.2 g, 87 % over two steps) as a colourless oil.

tert-butyl 3-(bis(benzyloxy)phosphoryloxy)propyl(but-3-enyl)carbamate (**22b**)

Compound **22b** was synthesized from **21b** by following the general procedure G (colourless oil, 95 %).

tert-butyl 6-(bis(benzyloxy)phosphoryloxy)hexyl(but-3-enyl)carbamate (**22c**)

Compound **22c** was synthesized from **21c** by following the general procedure G (colourless oil, 95 %).

General Procedure H for the synthesis of compound 11a-11c

dibenzyl 2-(but-3-enylamino)ethyl phosphate (11a)
50% TFA in DCM (5 mL) was added slowly to a stirred solution of **22a** (1.0 g, 2.10 mmol) in dichloromethane (10 mL) at 0 °C. The reaction mixture temperature was increased and the resulting solution was stirred at room temperature for 2 h. Then the reaction mixture was diluted with the addition of DCM (20 mL) and treated with 30% NaHCO_3 solution (20 mL). The organic layer was washed with water and brine, dried over Na_2SO_4 and evaporated under vacuo. The crude residue was purified with flash column chromatography (dichloromethane-methanol (100:4)) to provide **11a** (0.34 g, 43 %) as a colourless oil.

dibenzyl 3-(but-3-enylamino)propyl phosphate (11b)

Compound **11b** was synthesized from **22b** using trifluoroacetic acid following the general procedure H (colourless oil, 37 %).

dibenzyl 6-(but-3-enylamino)hexyl phosphate (11c)

Compound **11c** was synthesized from **22c** using trifluoroacetic acid following the general procedure H (colourless oil, 39 %).

General Procedure I for the synthesis of compound 23a-23g

dibenzyl 2-(*N*-(but-3-enyl)-1-(4-phenylbutyl)-4-undec-10-enoyl-1*H*-pyrrole-2-carboxamido)ethyl phosphate (23a)

To a stirred solution of **10b** (0.50 g, 1.2 mmol) and **11a** (0.69 g, 1.4 mmol) in DMF (10 mL) was added HBTU (0.64 g, 1.7 mmol) and DIEA (8.6 mL, 4.8 mmol). The reaction was stirred at room temperature for 14 h. Then reaction mixture was diluted with ethyl acetate (20 mL) and washed with water (15 mL x 3) and the combined ethyl acetate layers were washed with brine and dried over Na_2SO_4 . The crude product was purified with flash column chromatography (hexane-ethyl acetate, (10:4)) to yield **23a** (0.73 g, 79 %) as a colourless oil.

dibenzyl 2-(*N*-(but-3-enyl)-1-(3-phenylpropyl)-4-undec-10-enoyl-1*H*-pyrrole-2-carboxamido)ethyl phosphate (23b)

Compound **23b** was synthesized from **10a** and **11a** by following the general procedure I (colourless oil, 66 %)

dibenzyl 3-(*N*-(but-3-enyl)-1-(3-phenylpropyl)-4-undec-10-enoyl-1*H*-pyrrole-2-carboxamido)propyl phosphate (23c)

Compound **23c** was synthesized from **10a** and **11b** by following the general procedure I (colourless oil, 92 %).

dibenzyl 3-(*N*-(but-3-enyl)-1-(4-phenylbutyl)-4-undec-10-enoyl-1*H*-pyrrole-2-carboxamido)propyl phosphate (23d)

Compound **23d** was synthesized from **10b** and **11b** by following the

general procedure I (colourless oil, 79 %).

dibenzyl 3-(*N*-(but-3-enyl)-1-(7-phenylheptyl)-4-undec-10-enoyl-1*H*-pyrrole-2-carboxamido)propyl phosphate (23e)

Compound **23e** was synthesized from **10c** and **11b** by following the general procedure I (colourless oil, 62 %).

dibenzyl 6-(*N*-(but-3-enyl)-1-(7-phenylheptyl)-4-undec-10-enoyl-1*H*-pyrrole-2-carboxamido)hexyl phosphate (23f)

Compound **23f** was synthesized from **10c** and **11c** by following the general procedure I (colourless oil, 72 %).

dibenzyl 6-(*N*-(but-3-enyl)-1-(4-phenylbutyl)-4-undec-10-enoyl-1*H*-pyrrole-2-carboxamido)hexyl phosphate (23g)

Compound **23g** was synthesized from **10b** and **11c** by following the general procedure I (colourless oil, 79 %)

General Procedure J for the synthesis of compound 24a-24g
(*E/Z*)-dibenzyl 2-(2,16-dioxo-19-(4-phenylbutyl)-3,19-diazabicyclo [15.2.1]icosa-1(20),6,17-trien-3-yl)ethyl phosphate (24a)

To the diene **23a** (0.25 g, 0.33 mmol) in anhydrous dichloromethane (20 mL) was added Grubb's 2nd generation catalyst (0.065 mmol). The mixture was heated to 45 °C and stirred for 30 min under a nitrogen atmosphere. An additional portion of Grubb's 2nd generation catalyst (0.065 mmol) was added and the solution was stirred for 10 h at 45 °C. Further, an additional portion of Grubb's 2nd generation catalyst (0.065 mmol) was added and stirred for 12 h. The reaction mixture was quenched by addition of activated charcoal and stirred for 6 h at room temperature. The reaction mixture was filtered through a pad of celite and concentrated under vacuo. The crude product was purified with flash column chromatography (hexane-ethyl acetate, (1:1)) to yield **24a** (0.137 g, 57 %) as a brown color oil.

(*E/Z*)-dibenzyl 2-(2,16-dioxo-19-(3-phenylpropyl)-3,19-diazabicyclo [15.2.1]icosa-1(20),6,17-trien-3-yl)ethyl phosphate (24b)

Compound **24b** was synthesized from **23b** following the general procedure J (brown colour oil, 45 %).

(*E/Z*)-dibenzyl 3-(2,16-dioxo-19-(3-phenylpropyl)-3,19-diazabicyclo [15.2.1]icosa-1(20),6,17-trien-3-yl)propyl phosphate (24c)

Compound **24c** was synthesized from **23c** following the general procedure J (brown colour oil, 46 %).

(*E/Z*)-dibenzyl 3-(2,16-dioxo-19-(4-phenylbutyl)-3,19-diazabicyclo [15.2.1]icosa-1(20),6,17-trien-3-yl)propyl phosphate (24d)

Compound **24d** was synthesized from **23d** following the general procedure J (colourless oil, 37 %).

(*E/Z*)-dibenzyl 3-(2,16-dioxo-19-(7-phenylheptyl)-3,19-diazabicyclo [15.2.1]icosa-1(20),6,17-trien-3-yl)propyl phosphate (24e)

Compound **24e** was synthesized from **23e** following the general procedure J (brown colour oil, 44 %).

(*E/Z*)-dibenzyl 6-(2,16-dioxo-19-(7-phenylheptyl)-3,19-diazabicyclo [15.2.1]icosa-1(20),6,17-trien-3-yl)hexyl phosphate (24f)

Compound **24f** was synthesized from **23f** following the general procedure J (brown oil, 49 %).

(*E/Z*)-dibenzyl 6-(2,16-dioxo-19-(4-phenylbutyl)-3,19-diazabicyclo [15.2.1]icosa-1(20),6,17-trien-3-yl)hexyl phosphate (24g)

Compound **24g** was synthesized from **23g** following the general procedure J (colourless oil, 58 %)

General Procedure K for the synthesis of compound 1 to 7

(*E/Z*)-2-(2,16-dioxo-19-(4-phenylbutyl)-3,19-diazabicyclo

[15.2.1]icosa-1(20),6,17-trien-3-yl)ethyl dihydrogen phosphate (1)

Compound **24a** (54 mg, 0.074 mmol) was dissolved in TFA/TIS/H₂O

(2:0.2:0.2 mL) and stirred for 2 h. The reaction mixture was concentrated under vacuo and residue was washed with cold diethyl ether. The resultant crude product was purified by RP-HPLC to give final compound **1** (11 mg, 26 %) as a colourless oil.

(*E/Z*)-2-(2,16-dioxo-19-(3-phenylpropyl)-3,19-diazabicyclo

[15.2.1]icosa-1(20),6,17-trien-3-yl)ethyl dihydrogen phosphate (2)

Compound **2** was synthesized from **24b** following the general procedure K (colourless oil, 31 %)

(*E/Z*)-3-(2,16-dioxo-19-(3-phenylpropyl)-3,19-diazabicyclo

[15.2.1]icosa-1(20),6,17-trien-3-yl)propyl dihydrogen phosphate (3)

Compound **3** was synthesized from **24c** following the general procedure K (colourless oil, 26 %).

(*E/Z*)-3-(2,16-dioxo-19-(4-phenylbutyl)-3,19-diazabicyclo

[15.2.1]icosa-1(20),6,17-trien-3-yl)propyl dihydrogen phosphate (4)

Compound **4** was synthesized from **24d** following the general procedure K (colourless oil, 28 %).

(*E/Z*)-3-(2,16-dioxo-19-(7-phenylheptyl)-3,19-diazabicyclo

[15.2.1]icosa-1(20),6,17-trien-3-yl)propyl dihydrogen phosphate (5)

Compound **5** was synthesized from **24e** following the general procedure K (colourless oil, 32 %).

(*E/Z*)-6-(2,16-dioxo-19-(7-phenylheptyl)-3,19-diazabicyclo

[15.2.1]icosa-1(20),6,17-trien-3-yl)hexyl dihydrogen phosphate (6)

Compound **6** was synthesized from **24f** following the general procedure K (colourless oil, 37 %).

(*E/Z*)-6-(2,16-dioxo-19-(4-phenylbutyl)-3,19-diazabicyclo

[15.2.1]icosa-1(20),6,17-trien-3-yl)hexyl dihydrogen phosphate (7)

Compound **7** was synthesized from **24g** following the general procedure K (colourless oil, 55 %).

***In vitro* porcine oocyte maturation**

Prepubertal porcine ovaries were obtained from a local slaughterhouse (Farm Story dodram B&F, um-sung, chungbuk, Korea). Cumulus-oocyte complexes (COCs) were obtained from follicles that were 3-6 mm in diameter using 18-gauge microneedles. Oocytes with evenly granulated cytoplasm and a compact surrounding cumulus mass were collected and washed three times with TL-HEPES-PVA medium (Tyrode's lactate-HEPES medium supplemented with 0.01% polyvinyl alcohol). After washing, 70–80 COCs were transferred into 500 mL of IVM medium (TCM-199; Invitrogen, Carlsbad, CA) supplemented with 20 ng/mL epidermal growth factor, 1 g/mL insulin, 75 g/mL kanamycin, 0.91 mM sodium pyruvate, 0.57 mM L-cysteine, and 10% (v/v) porcine follicular fluid. After 22 h of culture, the COCs were transferred into IVM medium without hormones and cultured for an additional 22 h at 38.5°C in an atmosphere containing 5% CO₂ and 100% humidity.

Parthenogenetic activation and *in vitro* culture (IVC)

After maturation (44 h), cumulus cells were removed by repeated pipetting in the presence of 1 mg/mL hyaluronidase for 2–3 min. Denuded oocytes were activated by an electric pulse (1.0 kV/cm for 60 ms) in activation medium (280 mM mannitol, 0.01 mM CaCl₂, and 0.05 mM MgCl₂), followed by 3 h of incubation in PZM3 medium containing 2 mM cytochalasin B. About 70–80 post-activation oocytes were cultured in 4-well dishes containing 500 mL of PZM3 for 168 h. Embryo culture conditions were maintained at 38.5°C in an atmosphere containing 5% CO₂ and 100% humidity.

Mouse Oocyte collection and the *in vitro* maturation procedure

All procedures with mice were conducted according to the Animal Research Committee guidelines of Chungbuk National University, Korea, and all animal manipulations and experimental protocols were approved

by the Animal Research Committee, Chungbuk National University, Korea. The 4 to 6 week-old imprinting control region (ICR) mice were sacrificed by cervical dislocation at 48 h after injected with 10 IU of pregnant mare's serum gonadotropin (PMSG, Daesung Biochemical, Daejeon, Korea) and germinal vesicle (GV) stage oocytes were collected from ovaries. Cumulus-free and intact-GV follicular oocytes were released from large antral follicles via puncture with a needle in the M2 medium (Sigma-Aldrich, St. Louis, MO, USA) with 60 µg/mL of penicillin and 50 µg/mL of streptomycin. All cell culture were maintained in the M16 medium (Sigma-Aldrich) at 37 °C in a humidified atmosphere containing 5% of CO₂. Cumulus cell-enclosed metaphase II-arrested eggs were obtained from mice of the same strain. The cumulus cell masses surrounding the eggs were removed by brief exposure to 300 IU/mL hyaluronidase in the M2 medium.

Immunostaining and confocal microscopy

For immunostaining of the microtubules, oocytes were fixed in 4% paraformaldehyde dissolved in phosphate-buffered saline (PBS) and then incubated in a membrane permeabilization solution (0.5% Triton X-100) for 1 h. Oocytes were incubated with anti-lectin-FITC and anti- α -tubulin-FITC (1:200, respectively) for 1 h, washed three times in wash buffer for 2 min, incubated with Hoechst 33342 (10 µg/mL in PBS) for 15 min, and washed three times. Samples were mounted onto glass slides and examined using a confocal laser scanning microscope (Zeiss LSM 710 META, Jena, Germany) using a 40x water immersion objective lens for fixed oocytes.

Chemical microinjection

GV stage oocytes were injected with various macrocyclic compounds at 300 µM in a 50% aqueous solution (w/v) of dimethyl sulfoxide. Macrocyclic compounds were injected into oocyte by means of an Eppendorf Femto Jet (Eppendorf AG, Hamburg, Germany) and a Nikon Diaphot ECLIPSE TE300 inverted microscope (Nikon UK Ltd., Kingston upon Thames, Surrey, UK) equipped with a Narishige MM0-202N hydraulic three-dimensional micromanipulator (Narishige Inc., Sea Cliff, NY, USA) and subjected to *in vitro* maturation as described above. As a control, the BG34 reagent^[9] with threonine residues instead of phosphothreonine was injected into oocytes at 300 µM.

Molecular modeling methods

All calculations were performed using Discover 2.98/InsightII with CVFF force field as described by Hagler, A. T.; Lifson, S.; Dauber, P. J. Am. Chem. Soc., 1979, 101, 5122. The crystal structure of PBD of Plk1 having a pThr mimetic-containing C₆H₅(CH₂)₈- group bound was used as the computational model (3RQ7.pdb). The synthetic inhibitor **4** was built from the coordinates of this pThr mimetic-containing C₆H₅(CH₂)₈- group as found in the crystal structure using the Builder module in Insight II. The computational complex model was solvated using a solvent sphere of water extending 30.0 Å around the phosphate atom. The system was initially minimized using 1000 steps of steepest decent and 3000 steps of conjugated gradient with a 19.0 Å non-bonded cutoff distance.

Notes

This manuscript was written with the contribution of all authors. All the authors have approved the final version of the manuscript. The authors declare no competing financial interest.

Acknowledgements

This work was partly supported by International Collaborative Research Program of Institute for Protein Research, Osaka University, ICR-15-05 (J.K.B.), National Research Council of Science & Technology (NST) grant CAP-16-03-KRIBB, (J.K.B.),

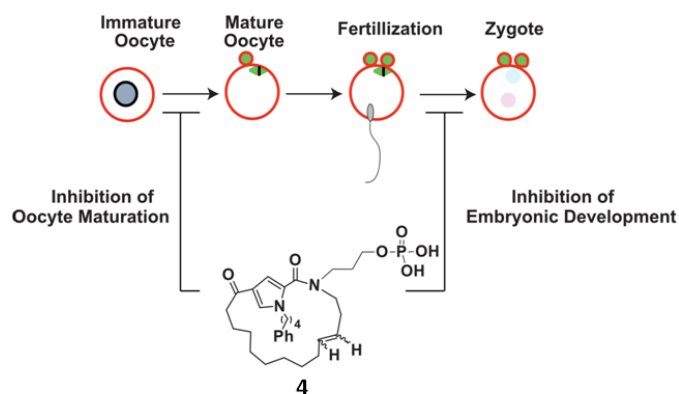
Korea Basic Science Institute Grant T36412 (J.K.B.) and the Next-Generation BioGreen 21 Program (PJ011126 and PJ011206), Rural Development Administration (N.H.K. and S.N.). The authors would like to thank Professor Kyoung Tai No for accessing the computational resources in his group.

Keywords: Oocyte maturation • Polo-like kinase 1 • Macrocyclic small molecule inhibitor • Contraceptive agent

References:

- [1] A. C. Gavin, M. Bösche, R. Krause, P. Grandi, M. Marzioch, A. Bauer, J. Schultz, J. M. Rick, A. M. Michon, C. M. Cruciat, M. Remor, C. Höfert, M. Schelder, M. Brajenovic, H. Ruffner, A. Merino, K. Klein, M. Hudak, D. Dickson, T. Rudi, V. Gnau, A. Bauch, S. Bastuck, B. Huhse, C. Leutwein, M. A. Heurtier, R. R. Copley, A. Edelmann, E. Querfurth, V. Rybin, G. Drewes, M. Raida, T. Bouwmeester, P. Bork, B. Seraphin, B. Kuster, G. Neubauer, G. Superti-Furga, *Nature*, **2002**, *415*, 141–147.
- [2] T. Berg, *Angew. Chem. Int. Ed.* **2003**, *42*, 2462–2481.
- [3] E. M. Phizicky, S. Fields, *Microbiol. Rev.* **1995**, *59*, 94–123.
- [4] J. L. Jia, Y. H. Han, H. C. Kim, M. Ahn, J. W. Kwon, Y. Luo, P. Gunasekaran, S. J. Lee, K. S. Lee, J. K. Bang, N. H. Kim, S. Namgoong, *Sci. Rep.* **2015**, *13*, 14626.
- [5] L. Otvos Jr, J. D. Wade, *Front Chem.* **2014**, *2*, 62.
- [6] F. M. Veronese, *Biomaterials*, **2001**, *22*, 405–417.
- [7] F. Liu, J. E. Park, W. J. Qian, D. Lim, M. Garber, M. B. Yaffe, K. S. Lee, T. R. Burke, Jr., *Nat. Chem. Biol.* **2011**, *7*, 595–601.
- [8] R. N. Murugan, J. E. Park, D. Lim, M. Ahn, C. Cheong, T. Kwon, K. Y. Nam, S. H. Choi, B. Y. Kim, D. Y. Yoon, M. B. Yaffe, D. Y. Yu, K. S. Lee, J. K. Bang, *Bioorg. Med. Chem.* **2013**, *21*, 2623–2634.
- [9] R. N. Murugan, M. Ahn, W. C. Lee, H. Y. Kim, J. H. Song, C. Cheong, E. Hwang, J. H. Seo, S. Y. Shin, S. H. Choi, J. E. Park, J. K. Bang, *PLoS One*, **2013**, *8*, e80043.
- [10] M. Ahn, Y. H. Han, J. E. Park, S. Kim, W. C. Lee, S. J. Lee, P. Gunasekaran, C. Cheong, S. Y. Shin Sr, H. Y. Kim, E. K. Ryu, R. N. Murugan, N. H. Kim, J. K. Bang, *J. Med. Chem.* **2015**, *58*, 294–304.
- [11] G. Srinivasrao, J. E. Park, S. Kim, M. Ahn, C. Cheong, K. Y. Nam, P. Gunasekaran, E. Hwang, N. H. Kim, S. Y. Shin, K. S. Lee, E. Ryu, J. K. Bang, *PLoS One*, **2014**, *9*, e107432.
- [12] E. Marsault, M. L. Peterson, *J. Med. Chem.* **2011**, *54*, 1961–2004.
- [13] K. C. Chua, M. Pietsch, X. Zhang, S. Hautmann, H. Y. Chan, J. B. Bruning, M. Gütschow, A. D. Abell, *Angew. Chem. Int. Ed. Engl.* **2014**, *53*, 7828–7831.
- [14] S. Ahmad, A. Sutherland, *Org. Biomol. Chem.* **2012**, *10*, 8251–8259.
- [15] G. C. Vougioukalakis, R. H. Grubbs, *Chem. Rev.* **2010**, *110*, 1746–1787.
- [16] T. Krejcova, M. Smelcova, J. Petr, J-F. Bodart, M. Sedmikova, J. Nevorál, M. Dvorakova, A. Vyskocilova, I. Weinggartova, V. Kucerova-Chrpova, E. Chmelikova, L. Tumova, F. Jilek, *PLoS One* **2015**, *10*, e0116964.
- [17] S. Namgoong, N. H. Kim, *Cell Cycle* **2016**, *15*, 1830–1843.
- [18] P. Solc, T. S. Kitajima, S. Yoshia, A. Brzakova, M. Kaido, V. Baran, A. Mayer, P. Samalova, J. Motlik, J. Ellenberg, *PLoS One* **2015**, *10*, e0116783.
- [19] K. Jeong, J. Y. Jeong, H. O. Lee, E. Choi, H. Lee, *Dev. Biol.* **2010**, *345*, 34–48.

Entry for the Table of Contents



Text for Table of Contents: Plk1 plays vital roles in fertilization and the inhibition of Plk1 hinders the oocyte maturation. We synthesized pyrrole based macro cyclic compounds which inhibited the oocyte maturation and affected the embryonic development potential of porcine oocytes. Besides, the most potent macrocyclic compound, **4** displayed enhanced cell penetration towards cell membrane. Further, investigation of this compound treated mouse oocytes showed impaired spindles, confirmed the inhibition of Plk1.